

Graphic representation of the synthesis results in a telecommunication-filter design suite

Ivan V. Litovski and Vančo B. Litovski

Abstract—In the telecommunication-filter design suit an important activity is to visualize the analog prototype transfer function (TF) synthesis results. That allows the designer to verify its design and to generate documents related to the proper phase of the design process. In this paper part of the \mathcal{RM} software will be described that performs generation of frequency and time domain responses given the TF of a filter. Programs for amplitude, attenuation, phase, and group delay responses will be described for the frequency domain encompassing low-pass, band-pass, band-reject, high-pass and all-pass filters. Programs for drawing the time domain responses including Dirac and Heaviside excitations will be described for low-pass filters only. A main program enabling repetitive use of the TF analysis data for generation different drawn characteristics will be described too.

Index Terms—Filter design, graphics, time domain, frequency domain

I. INTRODUCTION

Telecommunication filters are perpetual challenge for the designers since the very start of the technology [1] [2]. Having an integrated design tool that covers all phases of the design for the most of popular technologies (Passive LC, active RC, active SC and digital IIR) is a challenge above all. It is our intention to develop such a system. Here we do report some of the results already achieved.

As depicted in Fig. 1., the design process encompasses several phases every and each of them needing a verification tool. Here we describe a small segment of a design system named \mathcal{RM} which is devoted to the verification of the synthesis process of the transfer function in the s -domain. It covers frequency and time domain characterization of the synthesis process for both baseband and transformed functions. The activities described in this paper are marked by proper gray background in the "graphic verification" boxes of Fig. 1.

The paper consists of two main parts. In the second section we will give a complete set of mathematical expressions used for the computations for both frequency and time domain. Than, in the third section we will select a low-pass transfer function and illustrate the results that may be produced by the \mathcal{RM} software in cases of low-pass, high-pass, band-pass and band-stop transfer functions, the later three obtained by proper transformation during the synthesis process.

Note, to the \mathcal{RM} software it is irrelevant the way of how the input data for drawing were generated.

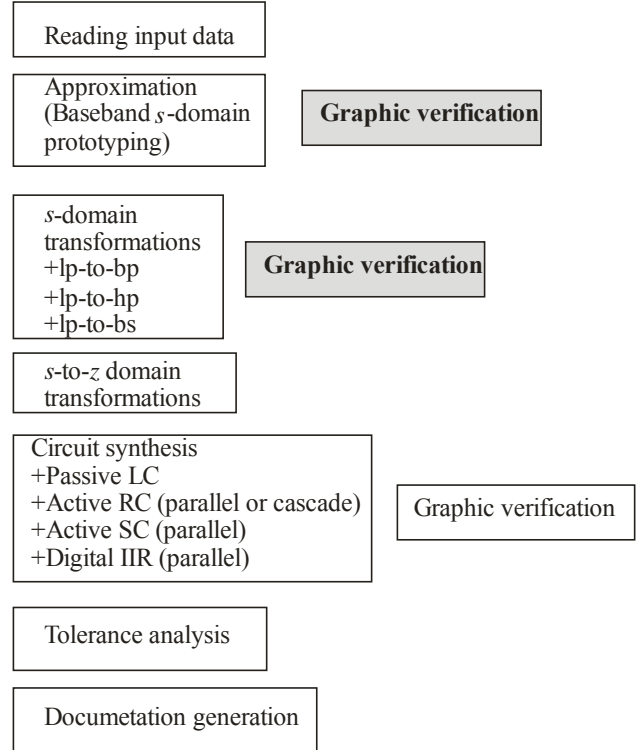


Figure 1. The filter design suite

II. COMPUTATIONS

We will first give the formulae used for the computation implemented in generation the graphics. The transfer function (TF) of a filter may be expressed as follows:

$$(1) \quad T(s) = A_0 \cdot \frac{\prod_{i=1}^m (s - z_i)}{\prod_{i=1}^n (s - p_i)}$$

Here s is the complex frequency: $s = \sigma + j\omega$. The imaginary part of the complex frequency is usually referred to as the real angular frequency while here the word "real" will be omitted. It is related to the frequency of the sinusoidal signal by: $\omega = 2\pi f$. Note, normalized frequencies will be used in the rest of the text. These are the ones obtained by division of the frequency by a normalization constant here appropriately denoted by ω_n or f_n .

The zeros of the TF (or the transmission zeros) are denoted by $z_k = \alpha_k + j\beta_k$, $k=1,2,\dots, n$, while the poles of the TF

are denoted as $p_i = \gamma_i + j\delta_i$, $i=1,2,\dots,m$. m is the order of the filter and $m \geq n$.

Usually unity nominal gain is sought so that the constant A_0 is computed as follows. For low-pass filters and band-stop filters having the lower part of the pass-band as a normalization region, we use

$$(1a) \quad A_0 = \frac{\prod_{k=1}^n (0 - p_k)}{\prod_{i=1}^m (0 - z_i)}.$$

For band-pass filters we use:

$$(1b) \quad A_0 = \frac{\prod_{k=1}^n (1 - p_k)}{\prod_{i=1}^m (1 - z_i)}$$

assuming the center frequency of the pass-band is normalized to unity.

And, for high-pass filters and band-stop filters having the upper part of the pass-band as a normalization region we use

$$(1c) \quad A_0 = 1.$$

On the axis of real frequencies or for $s=j\omega$, the amplitude characteristic is computed as follows:

$$(2) \quad |T(s)|_{s=j\omega} = \left[T(s)T(-s)|_{s=j\omega} \right]^{1/2}$$

or

$$(3) \quad |T(s)|_{s=j\omega} = |T_0| \frac{\prod_{k=1}^n \left[\alpha_k^2 + (\omega - \beta_k)^2 \right]^{1/2}}{\prod_{i=1}^m \left[\gamma_i^2 + (\omega - \delta_i)^2 \right]^{1/2}}.$$

If semi-log drawings are used the amplitude characteristic is expressed in decibels according to:

$$(4) \quad A(\omega) = 20 \cdot \log \left\{ |T(s)|_{s=j\omega} \right\} \text{ [dB]},$$

while the attenuation characteristic is obtained from:

$$(5) \quad a(\omega) = 20 \cdot \log \left\{ \frac{1}{|T(s)|_{s=j\omega}} \right\} \text{ [dB]}.$$

The general expression for the phase characteristic is given by

$$(6) \quad \varphi(\omega) = \arg \left\{ T(s)|_{s=j\omega} \right\} = \frac{1}{2j} \ln \left[\frac{T(s)}{T(-s)} \right]_{s=j\omega}$$

or

$$(7) \quad \varphi(\omega) = \sum_{k=1}^n \arctg \left[\frac{\beta_k - \omega}{\alpha_k} \right] - \sum_{i=1}^m \arctg \left[\frac{\delta_i - \omega}{\gamma_i} \right].$$

The very computation of the phase angle deserves some additional attention. Namely, all four quadrants are to be considered in every single summand in the above expression. For example, if both the nominator and the denominator are negative, the summand vector is pointing to the third quadrant so that its contribution to the phase is calculated as: $\pi + \arctg \left(\left| \frac{\text{nominator}}{\text{denominator}} \right| \right)$.

The group delay is obtained from the following expression

$$(8) \quad \tau(\omega) = - \frac{d\varphi(\omega)}{d\omega} = \sum_{k=1}^n \frac{\alpha_k}{\alpha_k^2 + (\omega - \beta_k)^2} - \sum_{i=1}^m \frac{\gamma_i}{\gamma_i^2 + (\omega - \delta_i)^2}$$

The response to a Dirac pulse (or the *pulse response*) was calculated for functions having simple poles only by the formula:

$$(9) \quad h(t) = \sum_{i=1}^n \lim_{s \rightarrow p_i} \left\{ \frac{\prod_{k=1}^n (s - z_k)}{\prod_{\substack{r=1 \\ r \neq i}}^m (s - p_r)} e^{s \cdot t} \right\} = \sum_{i=1}^n \left\{ \frac{\prod_{k=1}^n (p_i - z_k)}{\prod_{\substack{r=1 \\ r \neq i}}^m (p_i - p_r)} [\cos(\gamma_i \cdot t) + j \cdot \sin(\delta_i \cdot t)] \right\}$$

The response to a step or Heaviside function is obtained from (9) but the transfer function is changed so that a new pole is added being located in the origin. In other words instead of (1) one will use

$$(10) \quad T'(s) = A_0 \frac{\prod_{k=1}^m (s - z_k)}{s \prod_{j=1}^n (s - p_j)}$$

which means that the number of summands in the second sum in (9) will be risen by one due to the new pole: $p_{n+1} = 0 + j0$.

The time domain responses were computed for low pass TFs only.

III. A CASE STUDY

A set of programs were written to calculate and draw the characteristics of the just synthesized filters.

First, a program named TF-ANALYSIS is to be activated to create data for drawing. It recognizes automatically the

type of the filter creating five categories: low-pass, band-pass, band-stop, all-pass, and high-pass. Then it creates tables necessary for the drawings along with some additional data expressing the properties of the filter. Fig. 2. depicts part of the TF-ANALYSIS's output file related to the frequency and step response of a low-pass filter. The poles and zeros of that filter were taken from [3] and will be consistently used throughout this paper.

```

n=6, m=8
zeroes:
sigma=[1]=0.000000 omega=[1]=1.729902
sigma=[2]=0.000000 omega=[2]=-1.729902
sigma=[3]=0.000000 omega=[3]=2.257123
sigma=[4]=0.000000 omega=[4]=-2.257123
sigma=[5]=0.745520 omega=[5]=0.433547
sigma=[6]=0.745520 omega=[6]=-0.433547
poles:
sigma=[1]=-0.112344 omega=[1]=1.251432
sigma=[2]=-0.112344 omega=[2]=-1.251432
sigma=[3]=-0.378511 omega=[3]=1.081092
sigma=[4]=-0.378511 omega=[4]=-1.081092
sigma=[5]=-0.590394 omega=[5]=0.648007
sigma=[6]=-0.590394 omega=[6]=-0.648007
sigma=[7]=-0.651984 omega=[7]=0.259692
sigma=[8]=-0.651984 omega=[8]=-0.259692

Residues in the poles
p1[ 1 ]=-0.107213 q1[ 1 ]=0.117566
p1[ 2 ]=-0.107213 q1[ 2 ]=-0.117566
p1[ 3 ]=-0.056528 q1[ 3 ]=-0.935549
p1[ 4 ]=-0.056528 q1[ 4 ]=0.935549
p1[ 5 ]=1.102760 q1[ 5 ]=4.054906
p1[ 6 ]=1.102760 q1[ 6 ]=-4.054906
p1[ 7 ]=-0.939018 q1[ 7 ]=-6.943934
p1[ 8 ]=-0.939018 q1[ 8 ]=6.943934
*****
The cut-off frequency defined by 5.000000 dB
is equal to 1.295625
*****
delay time (at 0.5)=7.034871
rise time (0.1-0.9)=2.230270
*****
The number of oscillations at the beginning
of the step response is=2
time=2.00 value of the extremum=0.015097
time=4.50 value of the extremum=-0.048887
*****
The number of oscillations at the end
of the step response is=11
time=9.534871 value=1.124995
time=12.034871 value=0.925926
time=14.534871 value=1.055869
time=17.034871 value=0.960861
time=19.534871 value=1.028600
time=22.034871 value=0.978794
time=24.534871 value=1.015970
time=27.034871 value=0.987934
time=29.534871 value=1.009116
time=32.134871 value=0.993160
time=34.634871 value=1.005170

```

Figure 2. Part of the report created by TF-ANALYSIS for a low-pass filter

The drawing program is written entirely in C++ language with use of the Eclipse development framework [4] and the graphics.h library [5]. Both are open source programs available to anyone.

To allow the designer to have as a complete overview of the synthesis results as he needs, a separate interactive program was developed for the low-pass filters, which allows for repetitive generation of different drawings while using the same TF analysis output file.

In the sequel we are depicting different drawing results obtained by the RM's graphic output for synthesis verification.

It is worth mentioning that, in general, the designer may control the width and the aspect ratio of the drawing. The examples below were created to fit into a two column paper as prescribed by ETRAN.

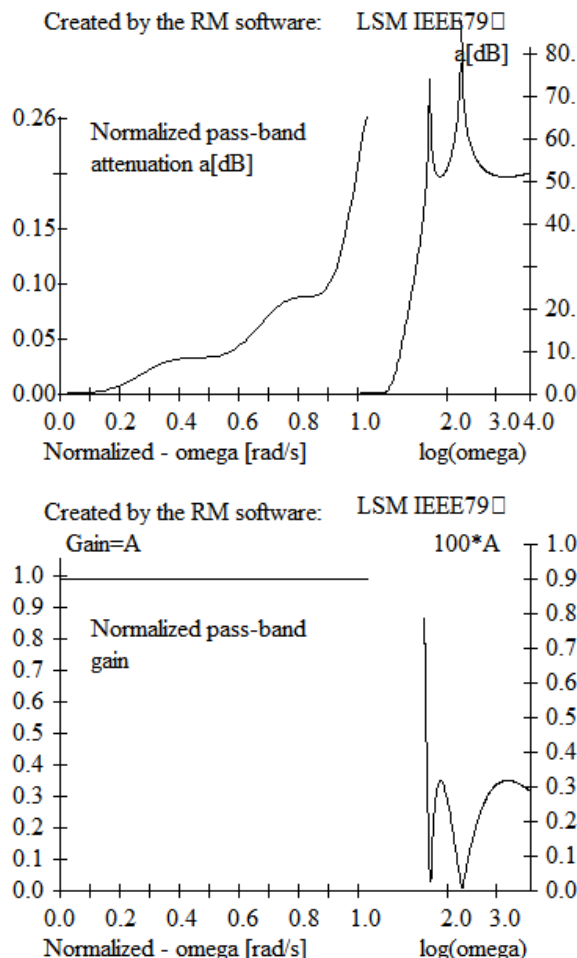


Figure 3. Amplitude characteristic (top attenuation, bottom gain)

Fig. 3. depicts two forms of presentation of the amplitude characteristic of a low pass filter. In the top part of the figure the attenuation is depicted. The term "normalized" used for the attenuation means that, before drawing, the gain at the origin was reduced to unity. In other words the value of A_0 in (1) was chosen so that $T(0)=1$. As can be seen the pass-band is depicted in semi-log fashion while the stop-band uses log-log diagram. Note, the maximum pass-band attenuation (a_{p-max}) is read by the program from the response table while the maximum normalized angular frequency (ω_{max}) and maximum attenuation (a_{s-max}) in the stop-band are supplied by the user. The bottom part of Fig. 3. is related to the amplitude characteristic with the difference that y-axis is linear both in the pass-band and in the stop-band. Note, since usually the values of the stop-band amplitude are small, the program calculates (based on the value of a_{s-max}) a multiplicative factor to enlarge the drawing. In Fig. 3. that multiplicative factor is shown to be 100.

Since the attenuation characteristic is of prime importance an opportunity is given to the designer to obtain the value of the normalized angular frequency at which the attenuation reaches a prescribed value. Implementation of that part of the program is illustrated in Fig. 2. where the frequency is shown at which the attenuation reaches 5 dB (which is arbitrary).

The next diagram (Fig. 4.) depicts the phase characteristic. Again two diagram may be created.

The first one depicts the phase in conjunction with the attenuation while the second is purely phase related. Instead of degrees, radians are drawn since that is the way how the $\arctg()$ function is working. The maximum value of the y-axis of the phase drawing is found from the analysis data while the frequency band in which the phase will be depicted is to be supplied by the designer.

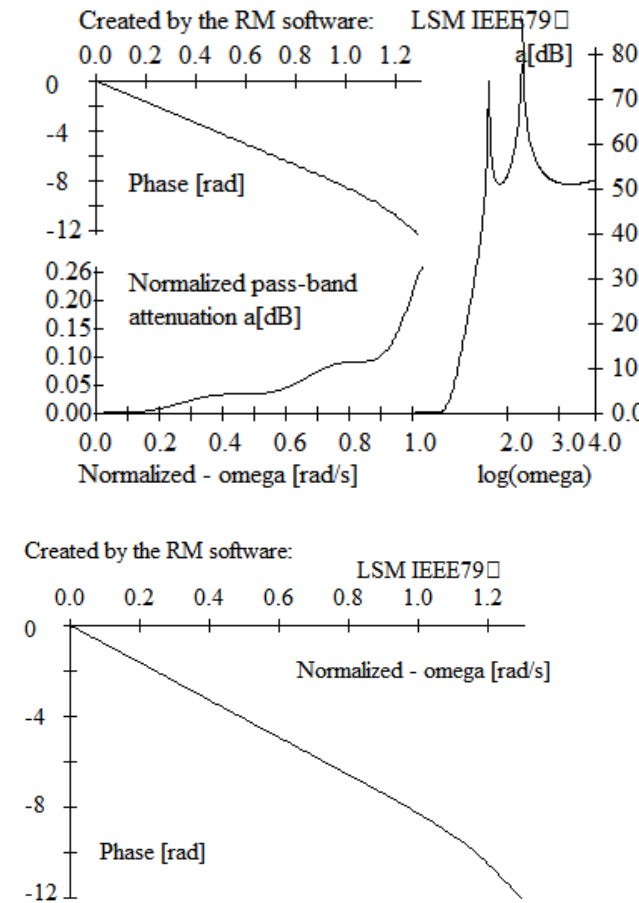


Figure 4. Phase characteristic (top attenuation and phase, bottom phase alone)

One may say practically all the same for the Fig. 5. where the group delay of the filter is depicted. In the top part of the figure the group delay is given in conjunction with the attenuation characteristic while in the bottom one it is depicted alone. Again, the maximum value of the delay at the diagram is found by search of the analysis table while the bandwidth is to be supplied by the designer.

It is important to note that the value of the group delay given in the drawings is normalized. That comes from the fact that the phase depicted in Fig. 4. was differentiated by the normalized frequency ($\omega = \omega_{\text{real}} / \omega_{\text{normalization}}$) where

$\omega_{\text{normalization}}$ usually is the filter's real cut-off frequency. That means that the real delay will be obtained after multiplication of the y-axis of the diagram of Fig. 4. by $\omega_{\text{normalization}}$.

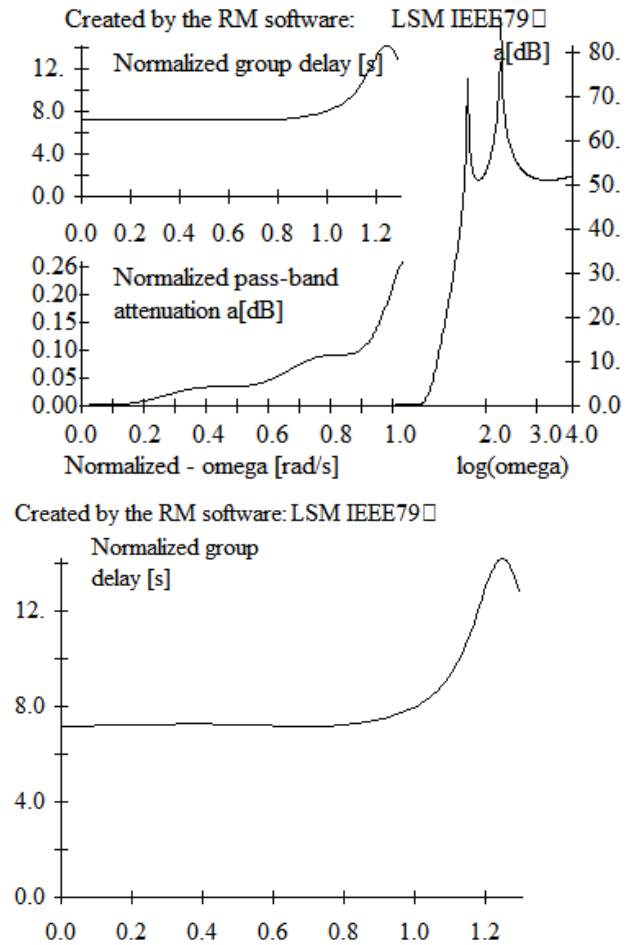


Figure 5. Group delay characteristic (top attenuation and group delay, bottom group delay alone)

The response to the Dirac impulse may be presented by two drawings also as depicted in Fig. 6. Here the time axis is normalized which is equivalent to the delay normalization described above.

Similarly, the Heaviside or the step response may be depicted in two ways as shown by Fig. 7. The same stands for the normalization.

Since the step response is of prime importance for characterization of a low-pass filter in the time domain, an opportunity is given to the designer to obtain the values of the coordinates of the extremal points of the step response. Implementation of that part of the program is illustrated in Fig. 2. where two tables are given one related to the oscillations at the beginning and the other to the oscillations to the end of the response. One may find from Fig. 2. that this filter exhibits an overshoot of approximately 12.5% and an undershoot of approximately 9.3%. The normalized delay-time of the filter (measured as the distance from the origin to the point when the response reaches 50% of its value at infinity) may be read from Fig. 2. to be approximately 7.0 s. In the same time the rise-time of the filter (measured as the time needed for the response to rise

from 0.1 to 0.9 of its final value) may be found to be approximately 2.2 s.

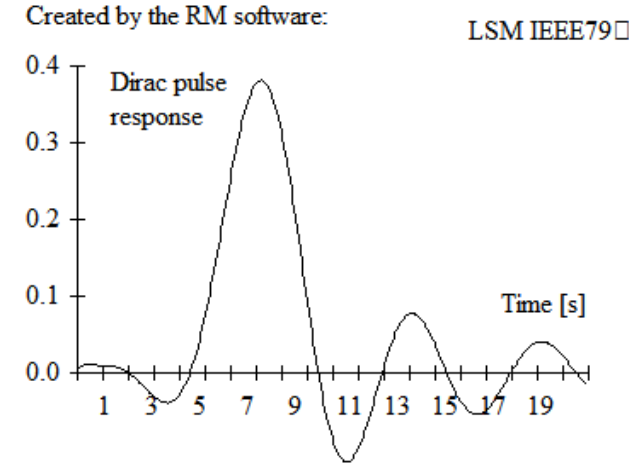
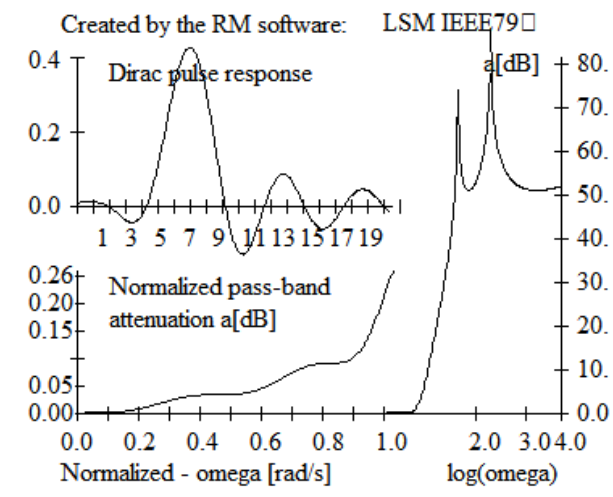


Figure 6. Dirac pulse response (top attenuation and pulse response, bottom pulse response alone)

That ends the description of the results and the available graphical presentation of a low-pass filter.

In the *RM* software a routine was written to perform transformations from low-pass to a high-pass, band-pass, or band-stop (or band-reject) filter function. The transformation is performed on the poles and zeroes of the low-pass function which, in the case of low-to-band transformations, leads to a solution of a second order algebraic equation with complex coefficients. We implemented our own procedure which is, in general, similar to the one described in [6].

Separate drawing programs were developed for the characteristics of the functions obtained by transformations. To begin with, Fig. 8. represents the attenuation characteristic of a high-pass filter obtained by transformation of the poles and zeros of the one studied as low-pass above. As can be seen the drawing is simply inverted. The main difference is in the fact that now the pass-band is infinite so that one needs both: to use logarithmic scale and to limit the maximum frequency which will be presented on the drawing. The last one is supplied by the designer. The stop-band is taken in geometric symmetry. So, if the pass-band is drawn up to $\omega=5$ rad/s, the stop-band will be drawn from $\omega=0.2$ rad/s.

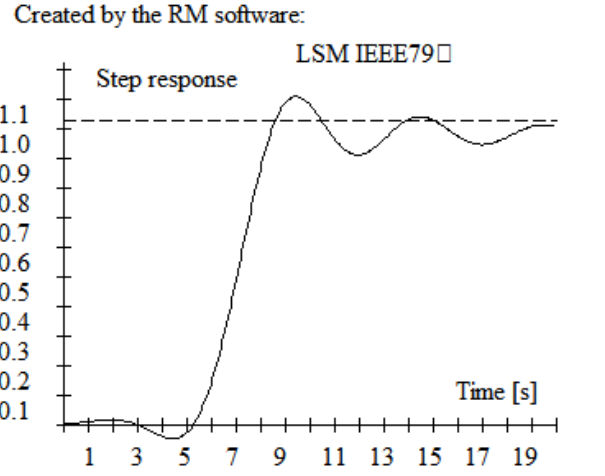
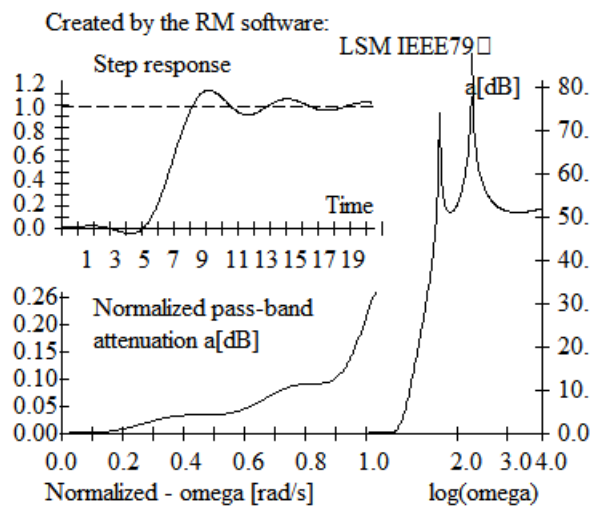


Figure 7. Heaviside response (top attenuation and pulse response, bottom step response alone)

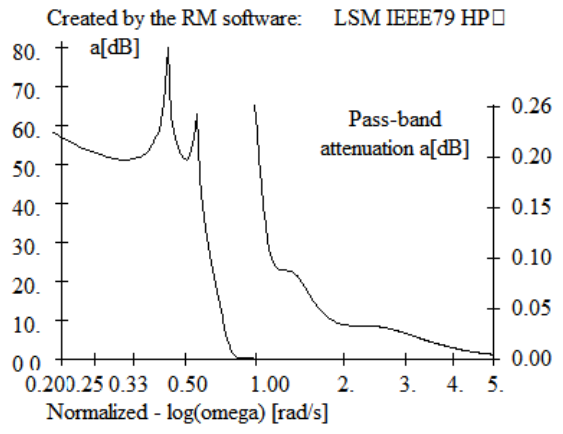


Figure 8. Attenuation characteristic of the high-pass filter

Fig. 9 depicts the attenuation characteristic of a filter obtained by low-pass to band-pass transformation of the same prototype filter. It was created so that its new pass-band to be half of the carrier frequency i.e. its relative bandwidth is $BW_r=0.5$. In this figure the pass-band attenuation is shown in a different scale. Namely, the upper value of the pass-band drawing was restricted to 0.4 dB.

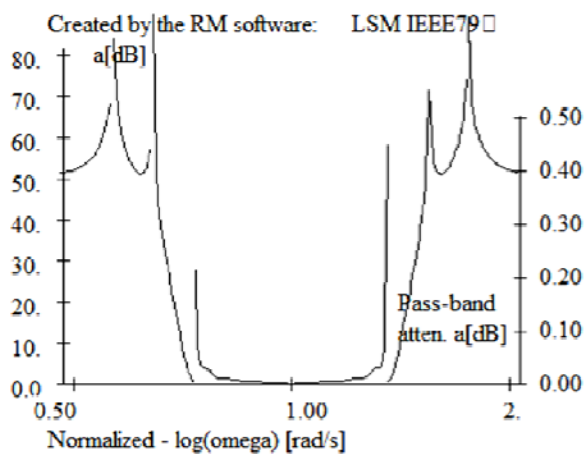


Figure 9. Attenuation characteristic of the band-pass filter ($BW_r=0.5$)

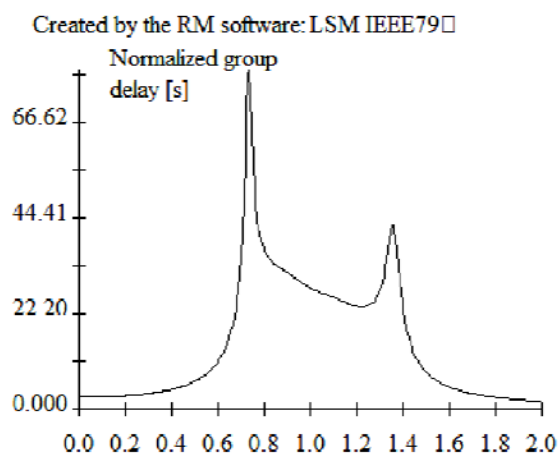


Figure 10. Group delay characteristic of the band-pass filter ($BW_r=0.5$)

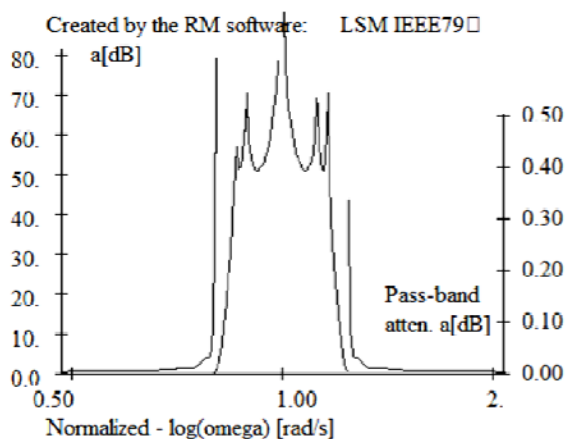


Figure 11. Attenuation characteristic of the band-reject filter ($BW_r=0.5$)

Fig. 10 depicts the group delay of the band-pass filter obtained by transformation as before. Note the linear scale on the x-axis. The diagram of Fig. 9. was considered to be too crowded so we decided to go with a separate drawing for the group delay in the band-pass case.

Finally, Fig. 11. depicts the attenuation characteristic of a band-stop filter obtained by transformation of the example prototype.

IV. CONCLUSION

Availability of a versatile and easily accessible tool for graphical presentation of the synthesis results is of crucial importance in both: the optimization and the documentation phase of the filter design. It was developed so that to enable multiple diagrams to be created after the same transfer function analysis enabling in the same time the parameters of the drawing to be accommodated depending on the users needs. A special value of these results is that they may be used for mutual verification with the final circuit-synthesis results by comparison with the results obtained by circuit or logic simulation.

REFERENCES

- [1] S. Humpherys, *The Analysis, Design, and Synthesis of Electrical Filters*, Prentice-Hall, 1970.
- [2] A. Williams, and F., Taylor, *Electronic Filter Design Handbook*, McGraw-Hill Professional, 4 edition, 2006.
- [3] V., Litovski, Synthesis Of Monotonic Passband Sharp Cutoff Filters With Constant Group Delay Response, *IEEE Trans. on Circuits and Systems*, ISSN: 1549-8328, Vol. CAS-26, No. 8, 1979, pp. 597-602.
- [4] -, <http://www.eclipse.org/>
- [5] -, <http://www.programmingsimplified.com/c/graphics.h>
- [6] P.R. Geffe, Design guide to active band-pass filters, *EDN (Electrical Design News)*, ISSN: 0012-7515, April 05, 1974, pp. 46-52.